2-D Quantum Transport Device Modeling by Self-Consistent Solution of the Wigner and Poisson Equations

Zhiyi Han, Neil Goldsman and Chung-Kai Lin
Department of Electrical Engineering, University of Maryland, College Park, MD 20742
Email: zyhan@glue.umd.edu, neil@glue.umd.edu Fax:+1-301-3149281 Phone:+1-301-405-3648

Abstract—**A new approach for simulating quantum transport in nanoscale semiconductor devices is presented. The method is based on the self-consistent solution of the Poisson and Wigner equations within a device. The spherical harmonic approach is used to transform the Wigner equation into a tractable expression. The results provide the distribution function and its averages throughout the device. The method has been applied to a MOSFET and a BJT. Inclusion of quantum effects reduces carrier concentrations near potential energy barriers leading to reduced terminal current.**

I. Introduction

Simulation of quantum effects has become increasingly important as device dimensions shrink below $0.1\mu m$, and gate oxide thicknesses reduce to only a few nanometers. Various methods have been proposed to account for quantum effects in device simulation [1]–[4].. These various approaches have their respective strengths. For example, the moment approaches can give quantum corrections to macroscopic quantities such as carrier concentration. However, they suffer from many of the same approximations as their semiclassical analogues. Furthermore, they do not provide a quantum distribution function. On the other hand, methods that employ the Wigner formalism can provide the quantum distribution function, but they usually rely on simplified phenomenological scattering terms to make their equations tractable for numerical solution. As a result, no single method has emerged as the approach of choice for modeling quantum phenomena in deep submicron and nanoscale electronics.

We have developed a new approach for modeling quantum transport in nanoscale semiconductor devices. The method is suitable for both 1-D and 2-D applications. It accounts in detail for both semiclassical and quantum transport. We start with the Wigner transport equation. To this equation we then add a semiclassical collision integral identical to the one used in the Boltzmann transport equation (BTE). This allows for the incorporation of elastic and inelastic scattering, including optical, acoustic phonon and ionized impurity scattering, which is critical to determining electron transport in semiconductors. Modeling is achieved by self-consistently solving Poisson equation with the Wigner equation of quantum transport. Below we show that the Wigner equation can be considered to be an extension of the semiclassical Boltzmann transport equation. We therefore solve the Wigner equation by extending the techniques that have already developed for the BTE, including the Spherical Harmonic expansion[5]–[7]. Extending the Spherical Harmonic methodology to the Wigner equation allows for the reduction of dimensionality, as well as for a rigorous treatment of collisions. The solution of the Wigner transport equation provides the Wigner function throughout the device, which is usually interpreted to be the quantum distribution function. From the Wigner function we directly obtain the quantum corrected carrier and current densities. We can also extract energy dependent phenomena including impact ionization and gate current.

The new approach has been applied to the simulation of a 2-D MOSFET, as well as a 1-D BJT. Results show corrections which are expected from quantum mechanical calculations, including reduction in electron concentrations in the vicinity of potential energy barriers. These barries include the MOSFET gate-oxide interface, the source-channel PN junction, as well as the BJT base-emitter junction. Calculated MOSFET current-voltage shows a small reduction in the drain current when compared to the semiclassical results.

II. Theory and Realization

The Wigner function $w(\vec{r},\vec{p},t)$ is defined as the Fourier transform of the product of two particle wavefunctions $\psi(\vec{r}\pm\vec{r'},t)$ separated in space by the position vector $\vec{r'}$:

$$w(\vec{r},\vec{p},t)=\frac{1}{\pi^3}\int e^{2i\vec{r'}\cdot\vec{p}}\psi^*(\vec{r}+\vec{r'},t)\psi(\vec{r}-\vec{r'},t)d\vec{r'} \quad (1)$$

By differentiating the Wigner function with respect to time, and employing the Schrödinger equation, the transport equation for the Wigner function can be derived[8]. In order to account for collisions, we separate the potential into one resulting from fields and barriers, and one

0-7803-6279-9/00/$10.00 © 2000 IEEE

due to scattering. The time variation of w due to scattering is then given in detail by the collision integral. So the steady state Wigner transport equation becomes:

$$\frac{\vec{p}}{m}\cdot\nabla_{\vec{r}}w - q\sum_{n=0}^{\infty}\frac{(-1)^{2n}\hbar^{2n}}{4^n(2n+1)!}(\nabla_{\vec{p}}\cdot\nabla_{\vec{r}})^{2n+1}V(\vec{r})w = \frac{1}{(2\hbar\pi)^3}\sum_j\int\left[w(\vec{r},\vec{p}')S_j(\vec{p}',\vec{p}) - w(\vec{r},\vec{p})S_j(\vec{p},\vec{p}')\right]d^3\vec{p}' \quad (2)$$

Where $\nabla_{\vec{p}}$ operates only on w, and $\nabla_{\vec{r}}$ operates only on the potential $V(\vec{r})$. The functions $S_j(\vec{p}',\vec{p})$ refer to scattering rates obtained from Fermi's golden rule. We include optical, acoustic and ionized impurity scattering. For $n=0$, the Wigner transport equation reduces to the Boltzmann transport equation. It can therefore be interpreted that the high order terms of the potential expansion give quantum correction to the BTE. The higher order term is proportional $\hbar^{2n}$, which quickly become negligible. In our work we retain the first two terms of the potential. To analyze semiconductor devices on the nanometer scale, while including the detailed effects of electronic interactions, we first change independent variables from momentum to wave vector using $\vec{p}=\hbar\vec{k}$. We now employ a device model which includes the Poisson equation (3), the Wigner equation (5), and the hole-current continuity equation (6).

$$\nabla^2_{\vec{\mathbf{r}}}V(\vec{\mathbf{r}}) = \frac{q}{\epsilon_s}\left[\int w(\vec{\mathbf{k}},\vec{\mathbf{r}},\mathbf{t})d\vec{\mathbf{k}} - p(\vec{\mathbf{r}},t) - D(\vec{\mathbf{r}})\right] \quad (3)$$

$$\frac{\partial w}{\partial t} - \frac{q}{\hbar}\sum_{n=0}^{1}\frac{(-1)^{2n}}{4^n(2n+1)!}(\nabla_{\vec{k}}\cdot\nabla_{\vec{r}})^{2n+1}V(\vec{r})w + \frac{\nabla_{\vec{k}}\varepsilon}{\hbar}\cdot\nabla_{\vec{r}}w = \left[\frac{\partial w}{\partial t}\right]_{coll} \quad (4)$$

$$\frac{\partial p(\vec{r},t)}{\partial t} + \nabla_{\vec{\mathbf{r}}}\cdot\left[\mu_p p(\vec{\mathbf{r}})\nabla_{\vec{\mathbf{r}}}\phi(\vec{\mathbf{r}}) + \mu_p V_t\nabla_{\vec{\mathbf{r}}}p(\vec{\mathbf{r}})\right] = R(\phi,n,p) - G_{ii}(n,p) \quad (5)$$

$V(\vec{r})$ is the potential; $p(\vec{r},t)$ is the hole concentration; $D(\vec{r})$ is the net ion concentration due to doping; $w(\vec{r},\vec{k},t)$ is the electron Wigner or quantum distribution function; ε is the energy; $\vec{r}$ is the position vector; ϵ_s is the silicon dielectric constant; μ_p is the hole mobility; $R(n,p)$ is the recombination rate; $G_{ii}(n,p)$ is the hole generation rate from impact ionization. and $qV(\vec{r})$ is the potential energy.

We now employ the spherical harmonic expansion method, which was previously developed for the BTE, and shown to agree with Monte Carlo and experiment[5], [7], [6], [9]

$$w(\vec{r},\vec{k}) = \sum_{l=0}^{\infty}\sum_{m=-l}^{l}w_l^m(\vec{r},\varepsilon)Y_l^m(\theta_k,\phi_k) \quad (6)$$

The spherical harmonics allow us to analytically evaluate the collision integral and reduce dimensionality, making the Wigner equation tractable for numerical solution. The goal now is to find the expansion coefficients, which are functions of the scalar ε instead of the vector $\vec{k}$. After considerable mathematical manipulation, for 1-Dimensional application, we obtain the following form for the Wigner transport equation.

$$v\left(\frac{\partial}{\partial x}+\frac{\partial\gamma}{\partial x}\frac{1}{\gamma}\right)\left(\sqrt{\frac{1}{3}}w_1\right)Y_0^0 + v\left(\frac{\partial}{\partial x}\sqrt{\frac{1}{3}}w_0\right)Y_1^0 + \frac{w_1}{\tau}Y_l^0 + [QM]_0Y_0^0 + [QM]_1Y_1^0 = \left[\frac{\partial w_0}{\partial t}\right]_{coll}Y_0^0 \quad (7)$$

Where $\gamma=\frac{\hbar^2k^2}{2m^*}$. The terms $[QM]_0Y_0^0$ and $[QM]_1Y_1^0$ represent the quantum corrections. The remaining terms are semiclassical in that they are identical to the semiclassical BTE as formulated using spherical harmonics.

We now project onto the spherical harmonic basis, transform our independent variable from momentum magnitude to energy, we obtain equations for the coefficients w_o and w_1:

$$Y_0^0 \;:\; v\left[\left(\frac{\partial}{\partial x}+\frac{\partial\gamma}{\partial x}\frac{1}{\gamma}\right)\left(\sqrt{\frac{1}{3}}w_1\right)\right] - \frac{q\hbar}{24\epsilon}\frac{\partial\rho}{\partial x}\left[\hat{K}_0\left(\frac{3}{5}\sqrt{\frac{1}{3}}w_1\right)\right] = \left[\frac{\partial w_0}{\partial t}\right]_{coll} \quad (8)$$

$$Y_1^0 \;:\; v\left(\frac{\partial}{\partial x}\sqrt{\frac{1}{3}}w_0\right) - \frac{q\hbar}{24\epsilon}\frac{\partial\rho}{\partial x}\left[\hat{K}_1\left(\frac{3}{5}\sqrt{\frac{1}{3}}w_0\right)\right] = \frac{-w_1}{\tau} \quad (9)$$

where

$$\hat{K}_0 = \frac{\partial^3}{(\hbar\partial k)^3} + \frac{2}{\hbar^3k}\frac{\partial^2}{\partial k^2} - \frac{2}{\hbar^3k^2}\frac{\partial}{\partial k} \quad (10)$$

and

$$\hat{K}_1 = \frac{\partial^3}{(\hbar\partial k)^3} + \frac{4}{\hbar^3k}\frac{\partial^2}{\partial k^2} \quad (11)$$

Substitute w_1 in equation (10) in equation (9), we obtain the following equation:

$$\frac{v}{3\gamma}\left\{\frac{\partial}{\partial x}\left[\gamma v\tau\left(\frac{\partial w_0}{\partial x}+\frac{q\hbar^2}{24\epsilon v}\frac{\partial\rho}{\partial x}\hat{K}w_0\right)\right]\right\} = \left[\frac{\partial w_0}{\partial t}\right]_{coll} \quad (12)$$

where $\hat{K}=\hat{K}_0+\hat{K}_1$.

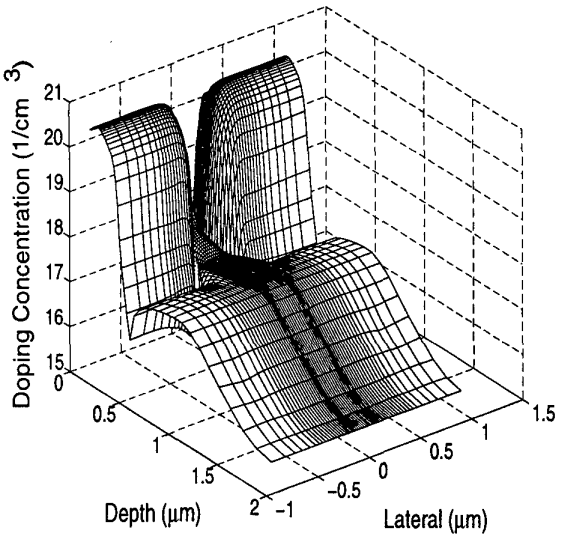

Fig.1 The doping profile of the simulated MOSFET.

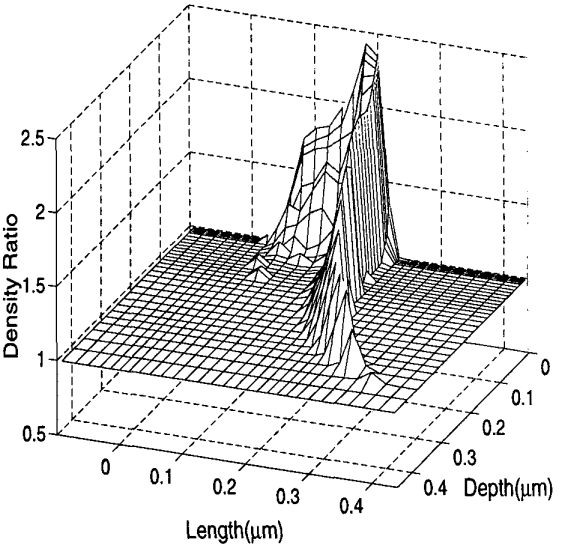

Fig. 2 Ratio of the simulated electron concentration: BTE/Wigner ($V_{GS} = 0.7V$, $V_{DS} = 0.5V$)

Through an analogous process, we can obtain the Wigner equation for 2-Dimensional applications:

$$\frac{v}{3\gamma}\left\{\frac{\partial}{\partial x}\left[\gamma v\tau\left(\frac{\partial w_0^0}{\partial x}+\frac{q\hbar^2}{24\epsilon v}\frac{\partial \rho}{\partial x}\hat{K}w_0^0\right)\right]+\right. \tag{13}$$

$$\left.\frac{\partial}{\partial y}\left[\gamma v\tau\left(\frac{\partial w_0^0}{\partial y}+\frac{q\hbar^2}{24\epsilon v}\frac{\partial \rho}{\partial y}\hat{K}w_0^0\right)\right]\right\}=\left[\frac{\partial w_0^0}{\partial t}\right]_{coll} \tag{14}$$

Equation (12) (equation (14) for 2-D) is discretized using a Scharfetter-Gummel like strategy, and then solved self-consistently with the Poisson and hole-current continuity equation. The coupled solution is a achieved using an iterative Gummel-like process.

III. Results

We solve the Wigner equation self consistently with the Poisson and hole-continuity equations for a 2-D MOSFET, as well as a 1-D BJT. The doping profile of the simulated MOSFET is shown in Fig. 1. The ratio of electron concentration calculated by the BTE to that obtained from the Wigner transport equation is shown in Fig. 2. We see the classical result predicts a factor of approximately two greater than the Wigner result near the interface. This is consistent with solutions to the Poisson-Schrodinger system. In the substrate the ratro is 1.0 indicating semiclassical transport in that region. Fig. 3 shows that the drain current found by Wigner is about 2 to 7 percent lower than that by BTE, which is again consistent with capacitance measurements and theory. Fig. 4 shows the doping profile of the simulated BJT. For the BJT we find that the electron concentration results obtained by BTE and Wigner equation. are similar deep in the emitter and collector where the potential is relatively constant. However, in Fig. 5 we show that near the emitter-base potential barrier, the electron density by obtained by the Wigner equation is lower than that by BTE. The difference reaches its peak of about 30% at $x = 0.7\mu m$ where the emitter-base depletion region and the potential barrier peak are located. We show the ratio of the classical distribution function to the quantum one in Fig. 6. The ratios of the classical to quantum distribution are very close to unity at the classical ohmic contacts, which is common for the two figures. This is because the potential in these regions is relatively constant indicating little quantum confinement. The ratios start to increase near $0.05\mu m$ and reach their peaks near $0.07\mu m$, where the barrier regions are located. Again, the calculations indicate that the quantum effect suppresses the carrier concentration in the vicinity of a barrier. The ratio of the distribution functions vary with energy. The quantum distribution functions predict less electrons at high energy than that predicted by the classical result. For the classical case, electrons can only surmount the base-emitter barrier from thermionic emission. As a result, classically only the higher energy electrons can be transported from the emitter into the base. However, quantum mechanics allows for tunneling of low energy electrons as well as injection of high energy electrons from thermionic emission. giving rise to a cooler distribution function.

Acknowledgements: We are grateful to Dr. Scott Yu and Dr. Surinder Singh for numerous discussions concerning the BTE and the Wigner equation, and to Intel Corporation for supporting the project.

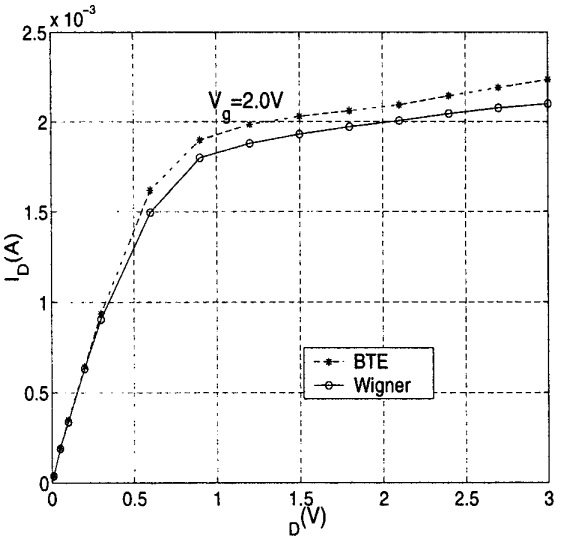

Fig. 3. The drain current comparison (Wigner vs. BTE).

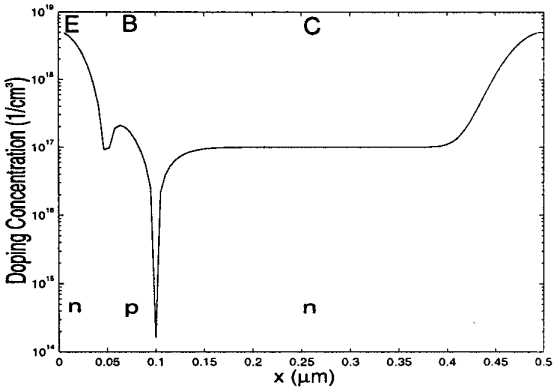

Fig. 4. The doping profile of the simulated BJT.

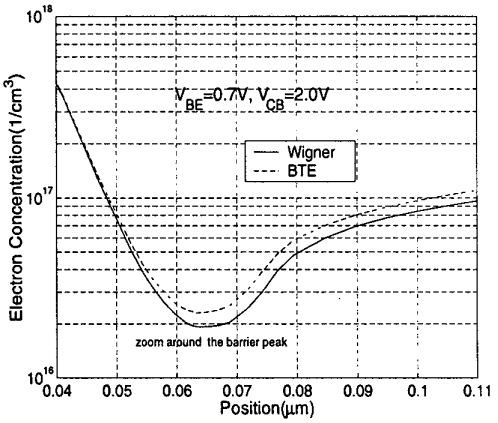

Fig. 5. Carrier concentration comparison near the emitter-base barrier peak (Wigner vs. BTE).

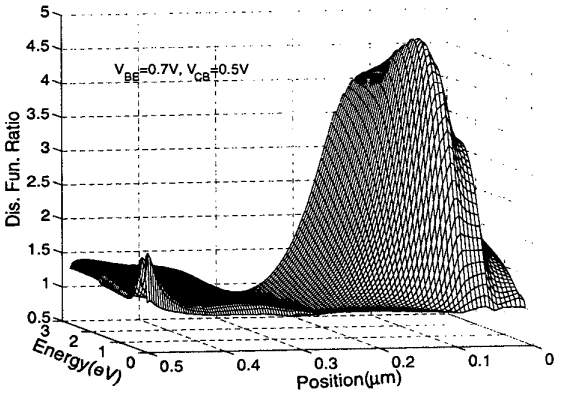

Fig. 6. Ratio of the semiclassical to the quantum distribution functions (semiclassical/quantum). The emitter contact is at $x = 0$. $V_{BE} = 0.7V$, $V_{CB} = 0.5V$.

References

[1] C. Gardner and C. Ringhofer, "Smooth quantum potential for the hydrodynamic model," *Phys. Rev.*, vol. E 53, pp. 157–167, 1996.

[2] D. K. Ferry and J. R. Barker, "Open problem in quantum simulation in ultra-submicron devices," in *Special Issue on Computational Electronics (IWCE-5)*, 1997.

[3] C. S. Rafferty, B. Biegel, M. A. Z. Yu, and R. W. D. J. Bude, "Multi-dimensional quantum effects simulation using a density-gradient model and script-level programming techniques," in *1998 INTERNATIONAL CONFERENCE ON SIMULATION OF SEMICONDUCTOR PROCESSES AND DEVICES*, 1998.

[4] A. Abramo, C. Fiegna, and P. Cassarini, "Quantum effects in the simulation of conventioal devices," in *1998 INTERNATIONAL CONFERENCE ON SIMULATION OF SEMICONDUCTOR PROCESSES AND DEVICES*, 1998.

[5] N. Goldsman, L. Henrickson, and J. Frey, "A Physics-Based Analytical/Numerical Solution to the Boltzmann Transport Equation for Use in Device Simulation," *Solid-State Electronics*, vol. 34, no. 4, pp. 389–396, 1991.

[6] K. A. Hennacy, Y.-J. Wu, N. Goldsman, and I. D. Mayergoyz, "Deterministic MOSFET Simulation Using a Generalized Spherical Harmonic Expansion of the Boltzmann Equation," *Solid-State Electronics*, vol. 38, pp. 1498–1495, 1995.

[7] W. Liang, N. Goldsman, I. Mayergoyz, and P. Oldiges, "2-dMOSFET modeling including surface effects and impact ionization by self-consistent solution of the Boltzmann, Poisson and hole-continuity equations," *IEEE Transactions on Elec. Dev.*, vol. 44, pp. 257–276, 1997.

[8] Y. S. Kim and M. E. Noz, *Phase Space Picture of Quantum Mechanics*. New Jersey: World Scientific, 1991.

[9] C.-H. Chang, C.-K. Lin, N. Goldsman, and I. D. Mayergoyz, "Spherical Harmonic Modeling of a 0.05μm Base BJT: A Comparison with Monte Carlo and Asymptotic Analysis," *VLSI Design*, vol. 8, pp. 147–151, 1998.